Seismic Design of a Structure Supported on Pile Foundation Considering Dynamic Soil-Structure Interaction

Yuji Miyamoto,[a] Katsuichiro Hijikata[b] and Hideo Tanaka[b]

It is necessary to predict precisely the structure response considering soil-structure interaction for implementation of performance-based design. Soil-structure interaction during earthquake, however, is very complicated and is not always taken into account in seismic design of structure. Especially pile foundation response becomes very complicated because of nonlinear interactions between piles and liquefied soil. In this paper pile foundation responses are clarified by experimental studies using ground motions induced by large-scale mining blasts and nonlinear analyses of soil-pile foundation-superstructure system.

INTRODUCTION

Vibration tests using ground motions induced by large-scale mining blasts were performed in order to understand nonlinear dynamic responses of pile-structure systems in liquefied sand deposits. Significant aspects of this test method are that vibration tests of large-scale structures can be performed considering three-dimensional soil-structure interaction, and that vibration tests can be performed several times with different levels of input motions because the blast areas move closer to the test structure. This paper describes the vibration tests and the simulation analyses using numerical model of nonlinear soil-pile foundation-superstructure system (Kamijho 2001, Kontani 2001, Saito 2002(a), 2002(b)).

VIBRATION TEST USING GROUND MOTIONS INDUCED BY MINING BLASTS

The vibration test method using ground motions induced by mining blasts is shown schematically in Figure 1. Vibration tests on a pile-supported structure in a liquefiable sand deposit were conducted at Black Thunder Mine of Arch Coal, Inc. Black Thunder Mine is

[a] Kajima Corporation, 6-5-30, Akasaka, Minato-ku, Tokyo 107-8502, Japan
[b] Tokyo Electric Power Company, 4-1, Egasaki-cho, Tsurumi-ku, Yokohama 230-8510, Japan

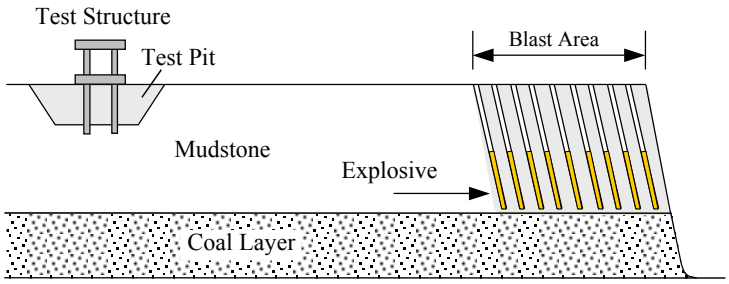

Figure 1. Vibration test method at mining site

one of the largest coalmines in North America and is located in northeast Wyoming, USA. At the mine, there is an overburden (mudstone layers) over the coal layers. The overburden is dislodged by large blasts called "Cast Blasts". The ground motions induced by Cast Blasts were used for vibration tests conducted in this research.

OUTLINES OF VIBRATION TESTS

A sectional view and a top view of the test pit and the pile-supported structure are shown in Figure 2 and Figure 3, respectively. A 12x12-meter-square test pit was excavated 3 meters deep with a 45-degree slope, as shown in Figure 2. A waterproofing layer was made of high-density plastic sheets and was installed in the test pit in order to maintain 100% water-saturated sand.

Outlines of the pile-supported structure are shown in Figure 4. Four piles were made of steel tube. Pile tips were closed by welding. Piles were embedded 70cm into the mudstone layer. The top slab and the base mat were made of reinforced concrete and were connected by H-shaped steel columns. The structure was designed to remain elastic under the

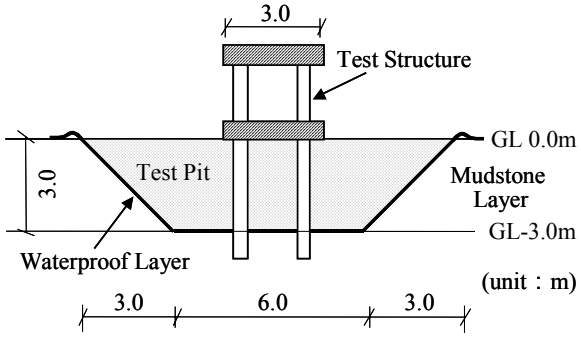

Figure 2. Sectional view of test pit

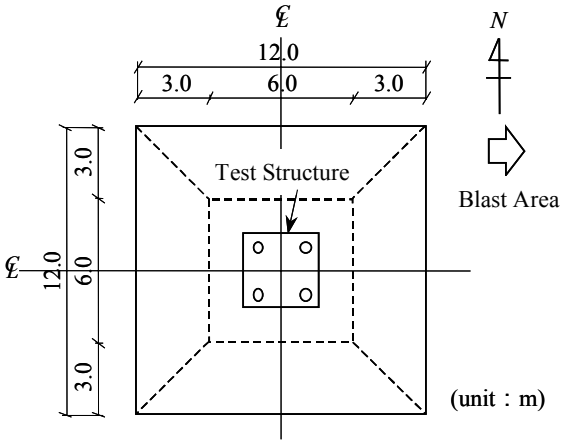

Figure 3. Top view of test pit

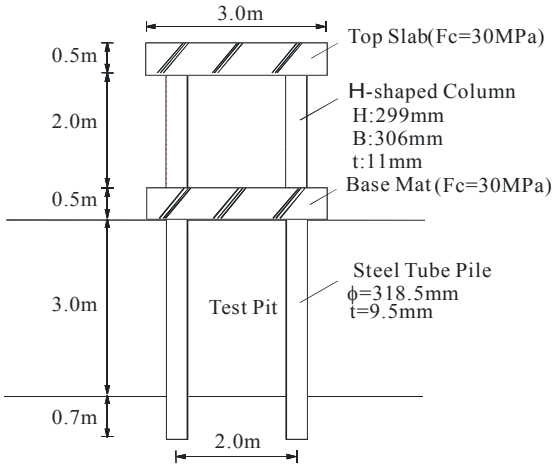

Figure 4. Pile-supported structure

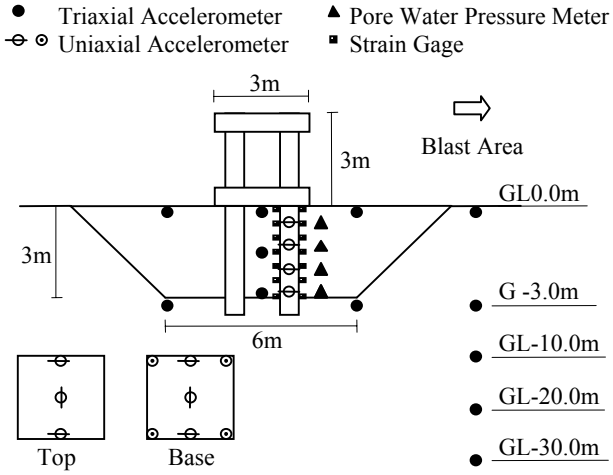

Figure 5. Instrumentation

conceivable maximum input motions, and the main direction for the structure is set in the EW direction. The construction schedule was determined so that the structure under construction received the least influence from mining blasts.

Instrumentation is shown in Figure 5. Accelerations were measured of the structure and one of the four piles. Accelerations in the sand deposit and free field adjacent to the pit were also measured in array configurations. Axial strains of the pile were measured to evaluate bending moments. Excess pore water pressures were measured at four levels in the test pit to investigate liquefaction phenomena.

PS measurements were conducted at the test site to investigate the physical properties of the soil layers. The shear wave velocity at the test pit bottom was about 200 m/s and this increased to 500 to 700 m/s with increasing depth. Core soil samples were collected for laboratory tests. The backfill sand was found near Black Thunder Mine. Great care was taken in backfilling the test pit with the sand, because the sand needed to be 100% water-saturated and air had to be removed in order to ensure a liquefiable sand deposit.

Figure 6. Test structure

Figure 6 shows the completed pile-supported structure and the test pit. The water level was kept at 10 cm above the

sand surface throughout seismic tests to prevent dry out of the sand deposit.

VIBRATION TEST RESULTS

Vibration tests were conducted six times. The locations of the blast areas for each test are shown in Figure 7. The blast areas were about 60m wide and 500m long. The results of the vibration tests are summarized in Table 1. The maximum horizontal acceleration recorded on the adjacent ground surface varied from 20 Gals to 1,352 Gals depending on the distance from the blast area to the test site. The closest blast was only 90m from the test site. These differences in maximum acceleration yielded responses at different levels and liquefaction of

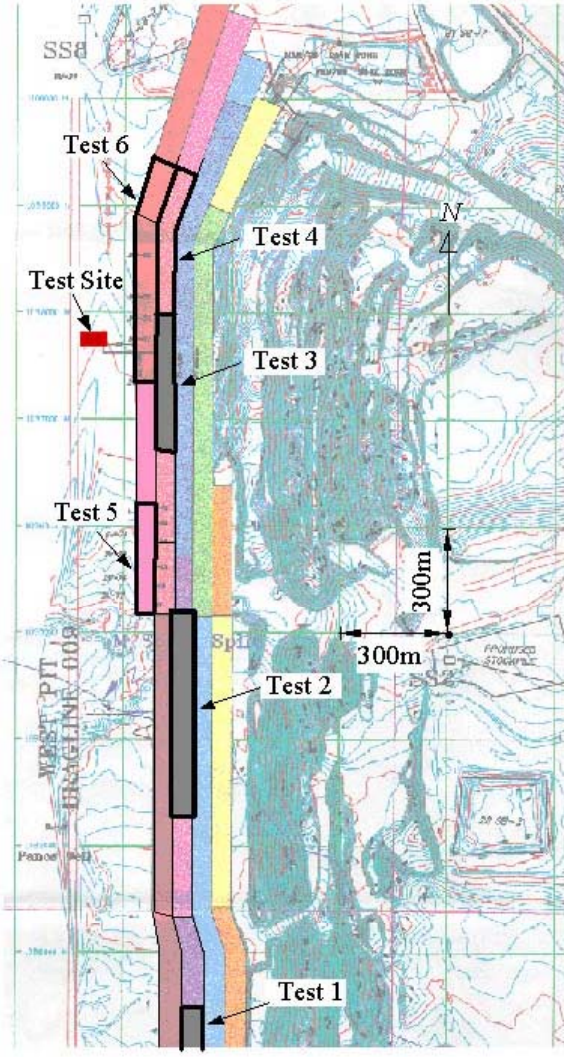

Figure 7. Locations of blasts in vibration tests

Table 1. Summary of vibration tests

Level of Input Motions	Test #	Distance (m) *	Max. Acceleration **		
			EW	NS	UD
Small	Test-1	3000	20	28	29
	Test-2	1000	32	84	48
Medium	Test-5	500	142	245	304
Large	Test-3	140	579	568	1013
	Test-4	180	564	593	332
Very Large	Test-6	90	1217	1352	3475

*: distance from blast area to test site
**: at the ground level of adjacent free field (Gals)

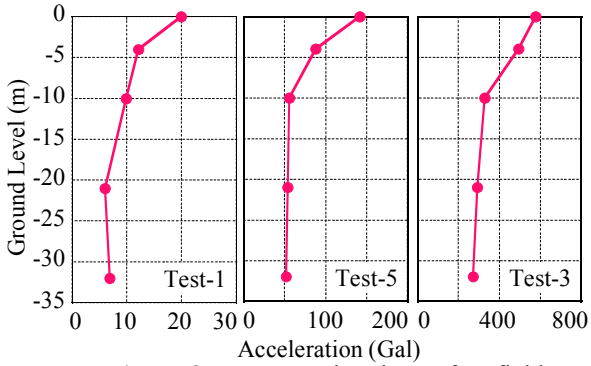

Figure 8. Max. acceleration at free field

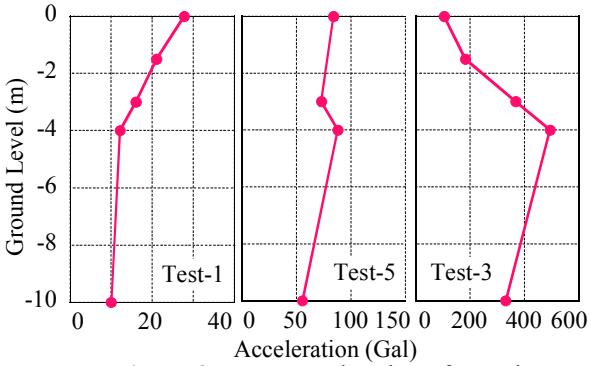

Figure 9. Max. acceleration of test pit

different degrees. Sand boiling phenomena were observed in the test pit with larger input motions.

In this paper, three tests (Test-1,5,3) indicated in Table 1 were chosen for detailed investigations, because those tests provided three different phenomena in terms of liquefaction of the sand deposit as well as in terms of dynamic responses of the structure. Horizontal accelerations in the EW direction are discussed hereafter.

DYNAMIC RESPONSES IN LIQUEFIED SAND DEPOSITS

The maximum accelerations recorded in the adjacent free field in vertical arrays are compared for three tests in Figure 8. The amplification tendencies from GL-32m to the surface were similar in the mudstone layers for three tests. The maximum accelerations recorded through the mudstone layers to the sand deposit are compared for these three tests in Figure 9. There was a clear difference among the amplification trends in the test pit. Test-1 showed a similar amplification trend to that of the mudstone layers as shown in Figure 8. Test-5 showed less amplification in the sand deposit. Test-3 showed a large decrease in

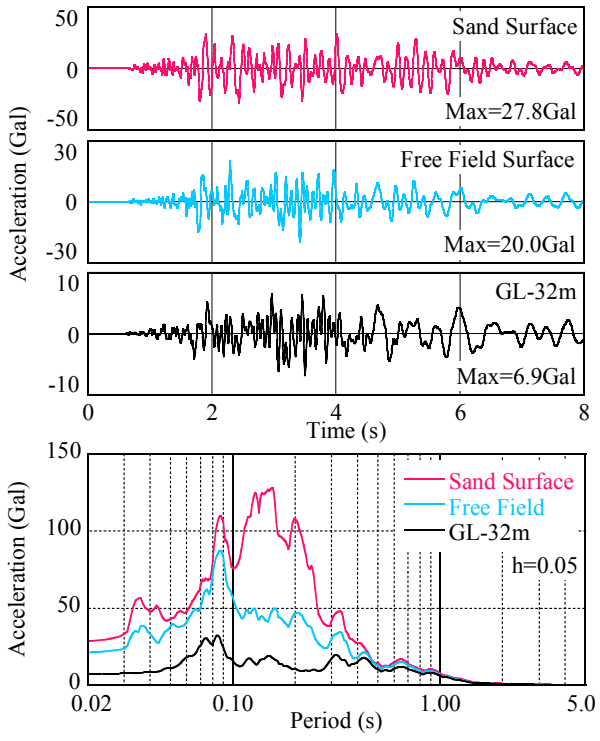

Figure 10. Acceleration records of Test-1 (Small Input Level)

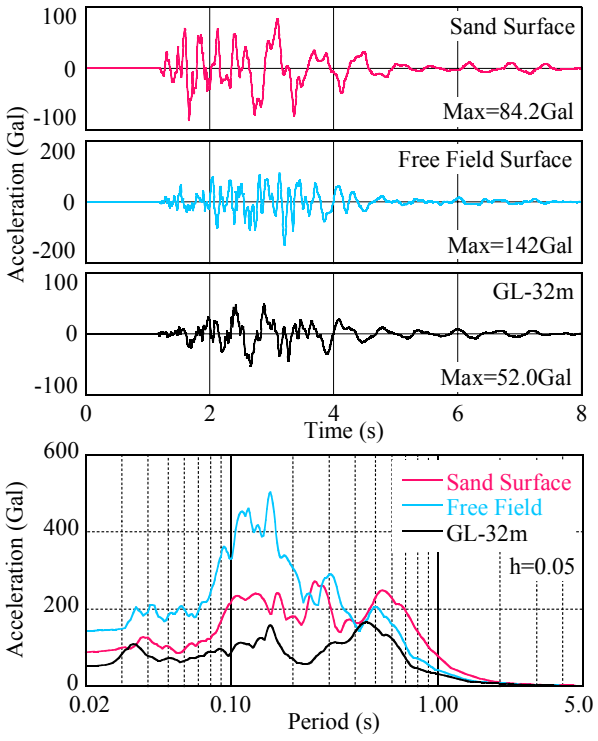

Figure 11. Acceleration records of Test-5 (Medium Input Level)

acceleration in the test pit because of severe liquefaction of the sand deposit.

Acceleration time histories at the sand surface, the free field surface and GL-32m are compared for Test-1 (Small Input Level) in Figure 10. The response spectra from these records are also shown in the figure. The same set of acceleration time histories and these response spectra are shown in Figure 11 for Test-5 (Medium Input Level) and in Figure 12 for Test-3 (Large Input Level).

As can be seen from Figure 10 for Test-1, over all the frequency regions, the responses at the sand surface were greater than those at the free field surface, and the responses at the free field surface were greater than those at GL-32m. From Figure 11 for Test-5, the responses at the sand surface and the free field surface were greater than those at GL-32m over all frequency regions. The responses at the sand surface became smaller than those at the free field surface for periods of less than 0.4 seconds due to in a certain degree of liquefaction of the sand. From Figure 12 for Test-3, the responses at the sand surface became much smaller than those at the free field surface and even smaller than those at GL-32m. These response reductions in the test pit were caused by extensive liquefaction over the test pit, because shear

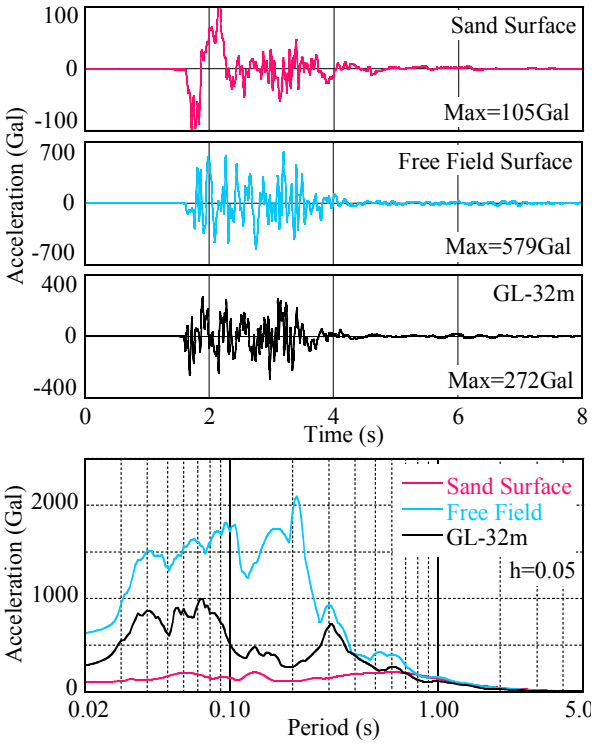

Figure 12. Acceleration records of Test-3 (Large Input Level)

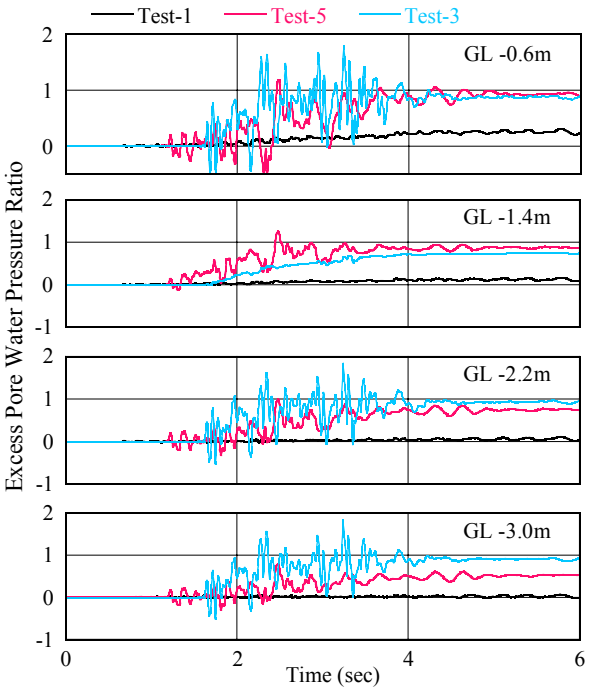

Figure 13. Measured time histories of excess pore water pressure ratio

waves could not travel in the liquefied sand.

Time histories of excess pore water pressure ratios are shown in Figure 13. The excess pore water pressure ratio is the ratio of excess pore water pressure to initial effective stress. In Test-1, the maximum ratio stayed around zero, which means that no liquefaction took place. In Test-5, the ratios rose rapidly, reaching around one at GL-0.6m and GL-1.4m after the main vibration was finished. Ratios at GL-2.2m and GL-3.0m were about 0.7 and 0.5. The measurement showed that the liquefaction region was in the upper half of the test pit. In Test-3, ratios at all levels rose rapidly, reaching around one, which indicates extensive liquefaction over the entire region. The large fluctuations in pressure records during main ground motions were caused by longitudinal waves.

Structure Responses Subjected to Blasts-Induced Ground Motion

Figure 14 compares the acceleration time histories at the top slab, the base mat and GL-3m of the pile for Test-1 (Small Input Level). The response spectra from these records are also shown. The same set of acceleration time histories and their response spectra are shown in Figure 15 for Test-3 (Large Input Level).

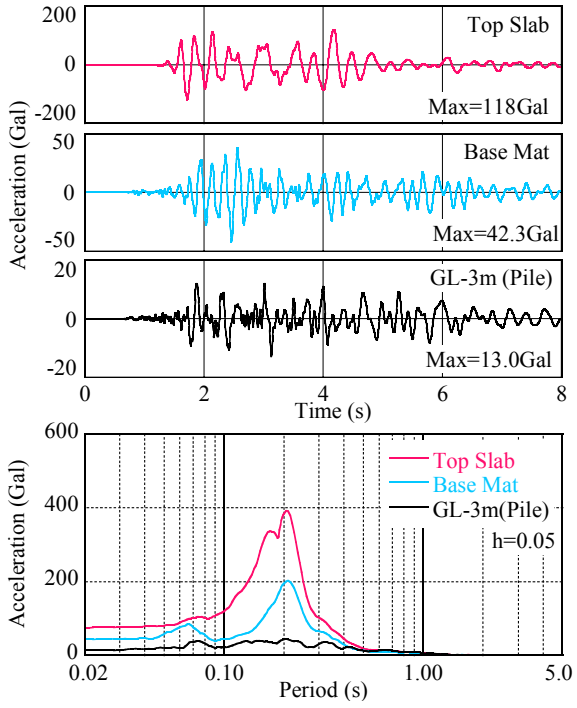

Figure 14. Acceleration records of test structure (Test-1 : Small Input Level)

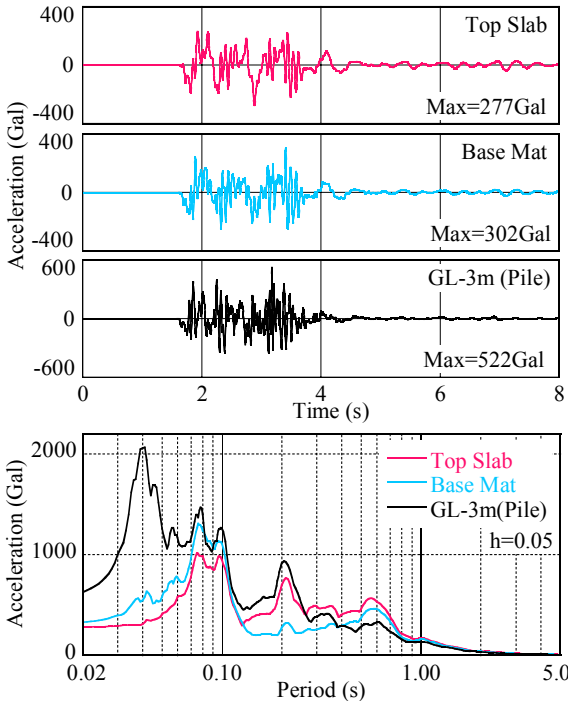

Figure 15. Acceleration records of test structure (Test-3 : Large Input Level)

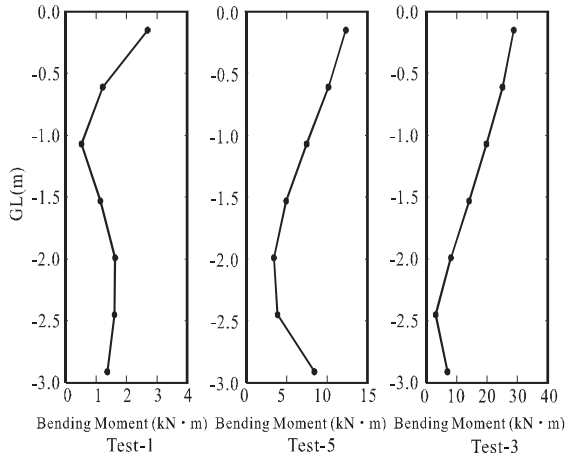

Figure 16. Maximum bending moments of pile

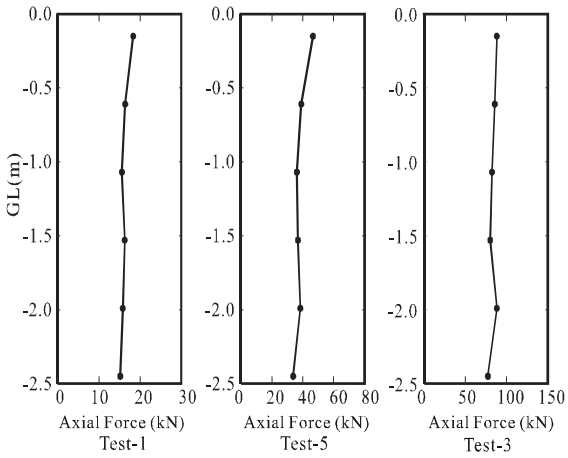

Figure 17. Maximum axial forces of pile

As can be seen from Figure 14 for Test-1, the maximum accelerations increased as motions went upward. For all frequency regions, the responses at the top slab were greater than those at the base mat, and the responses at the base mat were greater than those at GL-3m of the pile. The first natural period of the soil-pile-structure system was about 0.2 seconds under the input motion level of Test-1. For Test-3, the maximum accelerations decreased as motions went upward, which were different from those of Test-1. The responses at the top slab and the base mat became smaller than or similar to the responses at GL-3m of the pile. Compared with Test-1 results, it became difficult to identify peaks corresponding to natural periods of the soil-pile-structure system from response spectra diagrams. These results show that soil nonlinearity and liquefaction greatly influence the dynamic properties of pile-supported structures.

Measurement Results of Pile Stresses

The distributions of maximum pile stresses, bending moments and axial forces, are shown in Figures 16 and 17. The bending moment took its maximum value at the pile head for all cases. However, the moment distribution shapes differed and the inflection points of the curves moved downward in accordance with the input motion levels, in other words, the degrees of liquefaction in the test pit. However, the axial forces are almost the same regardless of the depth and similar tendencies are shown in all the test results.

ANALYSIS RESULTS

Figure 18 shows the analysis model for 3-D response of soil-pile-structure system. The soil response analysis is conducted by a 3D-FEM effective stress analysis method. The analyses were performed by a step-by-step integration method and employed a multiple shear mechanism model for the strain dependency of soil stiffness and Iai-Towhata model for evaluating the generation of excess pore water pressure (Iai 1992). Table 2 shows the soil constants. The shear wave velocity was measured by PS-Logging and the density of the saturated sand was measured by a cone penetration test. Soil nonlinearity was taken into account for all layers and Table 3 shows the nonlinear parameter for this simulation analysis. Figures 19 and 20 show the nonlinear properties and the liquefaction curve for the reclaimed sand, respectively. These curves are based on laboratory tests.

The super-structure is idealized by a one-stick model and the pile foundations are idealized by a four-stick model with lumped masses and beam elements. The lumped masses of the pile foundations are connected to the free field soil through lateral and shear interaction springs. A nonlinear vertical spring related to the stiffness of the supported layer is also incorporated at the pile tip, as shown in Figure 21. The initial values of the lateral and shear interaction soil springs of the pile groups are obtained using Green's functions by ring loads in a layered stratum and they are equalized to four pile foundations. The soil springs are modified in accordance with the relative displacements between soils and pile foundations and with the generation of excess pore water pressures (Miyamoto 1995).

3-D Responses of Liquefied Sand Deposits

Figure 22 shows the calculated time histories of the ground surface accelerations and the pore water pressure ratios. The amplitudes of the horizontal motions became smaller due to the generation of pore water pressure at time 2.5 seconds. However, the amplitude of the vertical motion was still large after 2.5 seconds. The analysis results are in good agreement with the test results.

Figure 23 shows the acceleration response spectrum of the ground surface in the EW direction. The blue line and the red line show the 3-D and 1-D analysis results respectively, and green line show the test results. All spectra have a first peak at 0.6 seconds, and the 3-D results are good agreement with the test result. Figure 24 shows the acceleration response spectrum of the ground surface in the UD direction. All spectra have a first peak at 0.3

seconds, and both of the 3-D and 1-D analysis results are in good agreement with the test result.

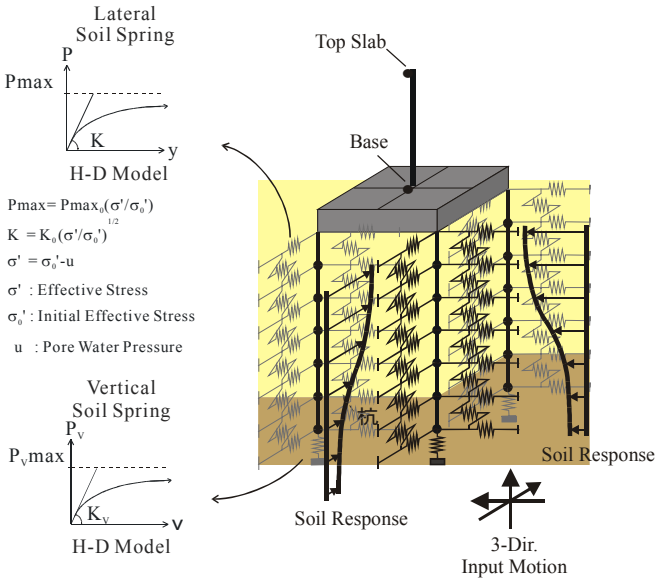

Figure 18. Three-dimensional analysis model for soil-pile-structure system

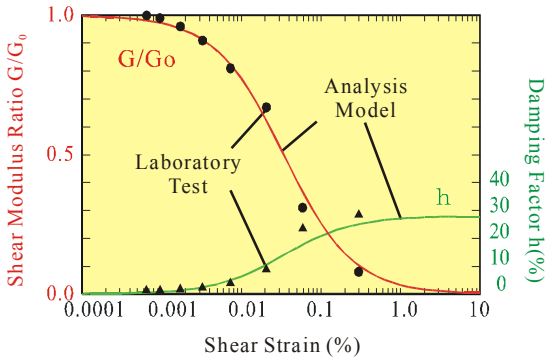

Figure 19. Nonlinear properties of reclaimed sand

Table 2. Soil properties for simulation analysis

Soil type	Thickness (m)	Unit Weight (kN/m³)	Vs (m/s)	Vp (m/s)
Sand (Test Bed)	3.0	18.9	80	1530
Clay	2.0	16.7	200	400
Mudstone	5.0	18.6	320	1240

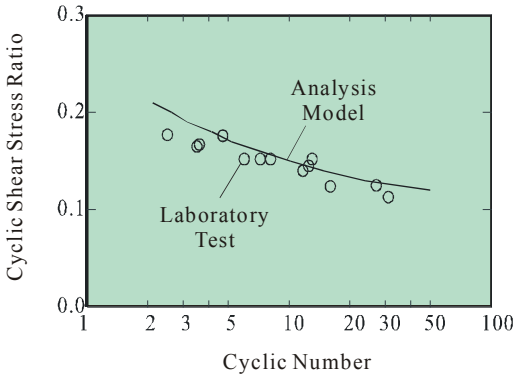

Figure 20. Liquefaction curve

Table 3. Nonlinear parameters

Reclaimed Sand

Reference Strain : 0.034% (G/G0=0.5)

Maximum Damping Factor : 28%

Liquefaction Parameter

W1=1.15, S1=0.005, P1=0.5,

P2=1.12, C1=1.6,

Phase Transformation Angle=28deg.

Clay and Mud Stone

Reference Strain : 0.17% (G/G0=0.5)

Maximum Damping Factor : 25%

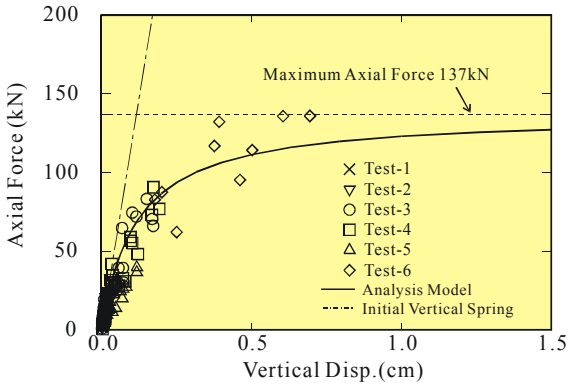

Figure 21. Relationship between vertical displacements and axial forces at pile head

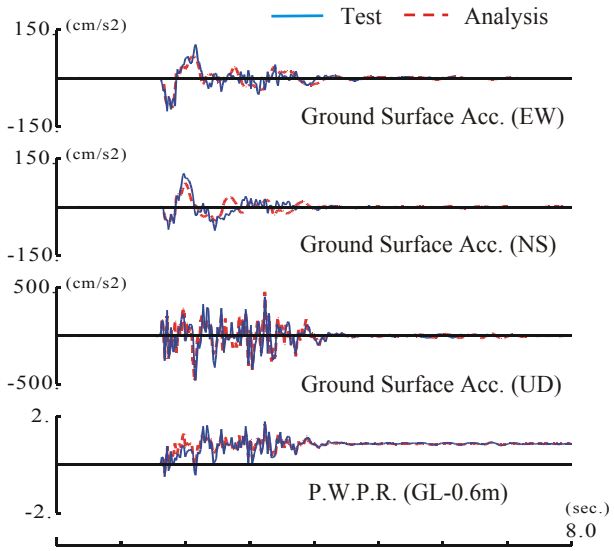

Figure 22. Comparisons of time-histories of ground surface accelerations and excess pore water pressure ratios at GL-0.6m for Test-3

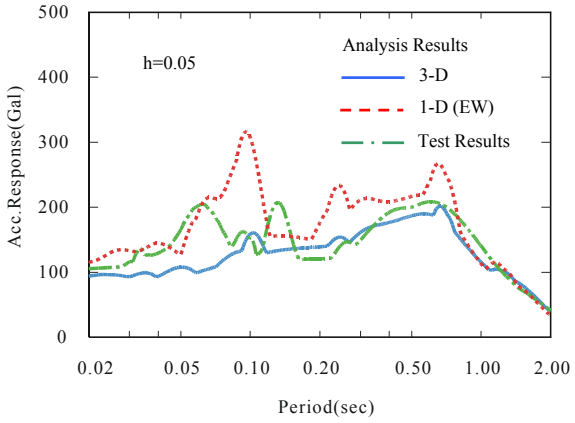

Figure 23. Comparisons of acceleration response spectrum of ground surface in EW direction

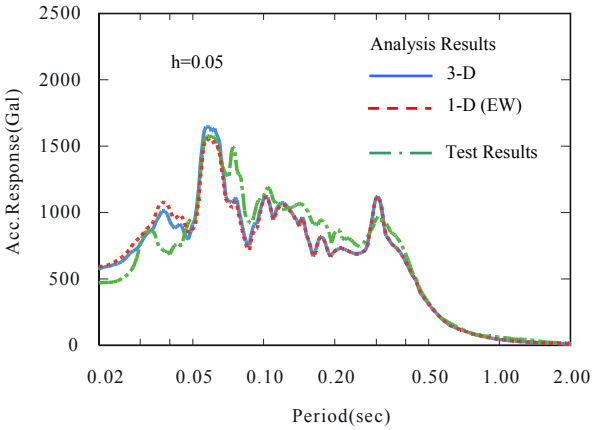

Figure. 24. Comparisons of acceleration response spectrum of ground surface in UD direction

Dynamic Responses for Test Structure

Figure 25 compares the calculated time-histories of acceleration for the test structure with the test results. The horizontal motions for the top slab of the test structure have almost the same amplitudes in the EW and NS directions, and are different from the records for ground surface shown in Figure 22. However, the vertical motion for the base mat of the test structure is almost the same as that for the ground surface shown in Figure 22. The analysis results are in good agreement with the test results not only in the horizontal directions but also in the vertical direction.

Figure 26 shows the displacement orbit in the EW and NS directions for the top slab and the ground surface. The horizontal motions of the ground surface had an almost circular orbit. On the other hand, the top slab had an elliptical orbit and amplitudes for the EW direction became larger than those for the NS direction due to the different vibration property of the test structure. The analysis results are in good agreement with the test results, and it is confirmed that this analysis method is applicable to evaluate the 3-D responses of pile-supported structures in liquefied sand deposits.

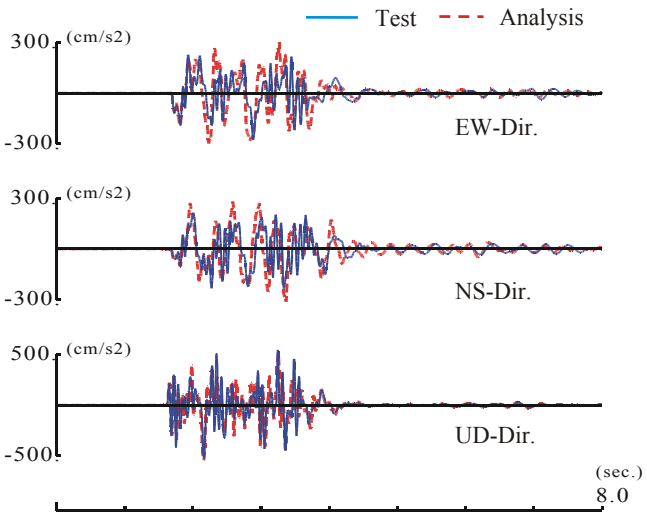

Figure 25. Comparisons of calculated time-histories of accelerations for top slab

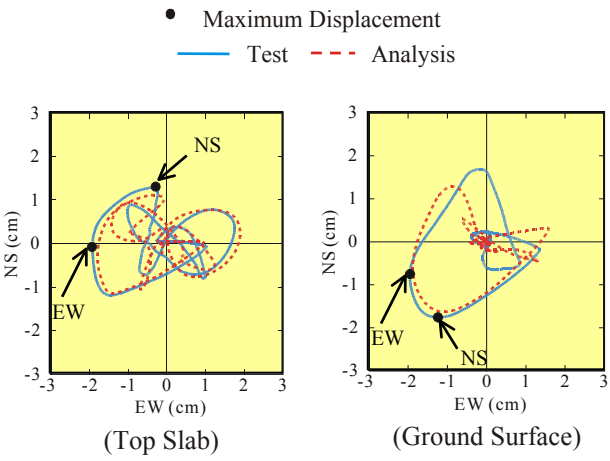

Figure 26. Relationship between displacements in EW and NS directions of top slab and ground surface

Bending Moments and Axial Forces for Pile Foundation

The distributions of maximum pile stresses, bending moments and axial forces, are shown in Figure 27. Bending moments became larger at the pile head as well as at the interface between the reclaimed sand and the supporting layer. The calculated maximum bending moments at pile heads are almost the same in the EW and NS directions, since the maximum acceleration of the superstructure were almost the same in both directions. The calculated

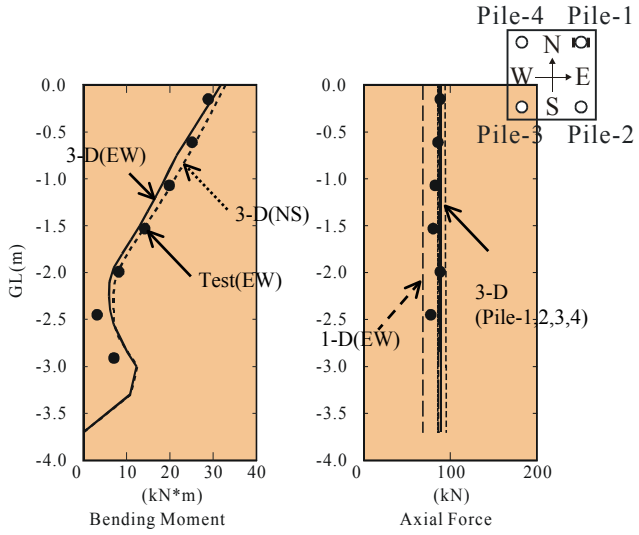

Figure 27. Comparisons of the maximum bending moments and the maximum axial forces by the location in pile arrangement

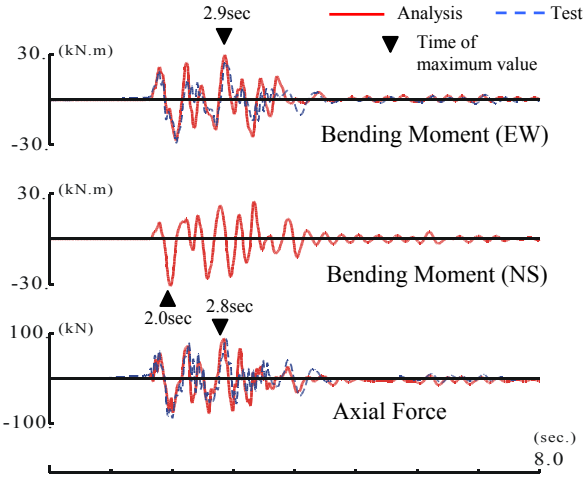

Figure 28. Comparisons of calculated time-histories of bending moments and axial force at pile head of Pile-1 (Axial force: compression(+), tensile(-))

maximum axial forces in the four piles are almost the same and about 90kN. The 1-D analysis result became smaller than the 3-D analysis results.

The time histories of the pile stresses at pile heads are shown in Figure 28. The analysis results are in good agreement with the test results, which indicates that this analysis method is applicable to evaluate pile stresses during liquefaction. The maximum bending moments occurred at 2.9 seconds in the EW direction and at 2.0 seconds in the NS direction. These times correspond closely with the superstructure responses, as shown in Figure 25. The time history of axial force at the pile head is similar with that of the bending moment in the EW direction, and it is different with that of the superstructure response in the UD direction shown in Figure 25.

CONCLUSIONS

Vibration tests were conducted of a pile-supported structure in a liquefiable sand deposit using ground motions induced by large mining blasts. Nonlinear responses of the soil-pile-structure system were obtained for various levels of liquefaction in the test pit. The vibration test method employed in this research was found to be very useful and effective for investigating the dynamic behavior of large model structures under severe ground motions. Simulation analysis results were in good agreement with the test results for the responses of the superstructure and pile stresses due to liquefaction. To evaluate the performance of pile foundation it is important to precisely predict pile response using nonlinear soil-pile foundation-superstructure system.

ACKNOWLEDGMENTS

We would like to express our deep appreciation to Dr. Aoyama, Professor Emeritus of the University of Tokyo, for his guidance throughout this experimental research. We would also like to thank Professor Robert Nigbor of University of Southern California, and the management and staff of Arch Coal's Black Thunder Mine for their assistance throughout the project.

REFERENCES

Kamijho, N., Saito, H., Kusama K., Kontani O. and Nigbor R., 2001. *Seismic Tests of a Pile-Supported Structure in Liquefiable Sand Using Large-Scale Blast Excitation, Proceeding of the 16th International Conference on Structural Mechanics in Reactor Technology (SMiRT-16),* Washington, Paper No.1488

Kontani, O., Tanaka, H., Ishida, T., Miyamoto, Y. and Koyamada, K., 2001. *Simulation Analyses of Seismic Tests of a Pile-Supported Structure in Liquefiable Sand Using Large-Scale Blast Excitation, Proceeding of the 16th International Conference on Structural Mechanics in Reactor Technology (SMiRT-16),* Washington, Paper No.1492

Saito, H., Tanaka, H., Ishida, T., Koyamada, K., Kontani, O. and Miyamoto, Y., 2002(a). *Vibration Test of Pile-Supported Structure in Liquefiable Sand Using Large-Scale Blast, -Simulation analyses for vibration tests of soil-pile-structure-, Journal of Structural and Construction. Engineering, Architectural Institute of Japan,* No. 557, pp.85-92 (in Japanese)

Saito, H., Tanaka, H., Ishida, T., Koyamada, K., Kontani, O. and Miyamoto, Y., 2002(b). *Vibration Test of Pile-Supported Structure in Liquefiable Sand Using Large-Scale Blast, - Outline of vibration tests and responses of soil-pile-structure -, Journal of Structural and Construction Engineering, Architectural Institute of Japan,* No. 553, pp.41-48 (in Japanese)

Iai, S., Matsunaga, Y. and Kameoka, T., 1992. *Strain Space Plasticity Model for Cyclic Mobility, Soils and Foundation,* Vol.32, No.2, pp.1-15

Miyamoto, Y., Sako, Y., Kitamura, E. and Miura, K., 1995. *Earthquake response of pile foundation in nonlinear liquefiable soil deposit, Journal of Structural and Construction Engineering, Architectural Institute of Japan,* No.471, pp.41-50 (in Japanese)